FULL PAPER

Ultrathin Flexible Graphene Film: An Excellent Thermal Conducting Material with Efficient EMI Shielding

Bin Shen, Wentao Zhai, and Wenge Zheng**

As the portable device hardware has been increasing at a noticeable rate, ultrathin thermal conducting materials (TCMs) with the combination of high thermal conductivity and excellent electromagnetic interface (EMI) shielding performance, which are used to efficiently dissipate heat and minimize EMI problems generated from electronic components (such as high speed processors), are urgently needed. In this work, graphene oxide (GO) films are fabricated by direct evaporation of GO suspension under mild heating, and ultrathin graphite-like graphene films are produced by graphitizing GO films. Further investigation demonstrates that the resulting graphene film with only ≈8.4 μm in thickness not only possesses excellent EMI shielding effectiveness of ≈20 dB and high in-plane thermal conductivity of ≈1100 W m^{-1} K^{-1}, but also shows excellent mechanical flexibility and structure integrity during bending, indicating that the graphitization of GO film could be considered as a new alternative way to produce excellent TCMs with efficient EMI shielding.

1. Introduction

Recently, portable device hardware, represented by the popularity of smartphone and tablet PCs, has been increasing at a noticeable rate. However, electronic components (such as high speed processors) in them would generate significant heat emissions and create undesirable electromagnetic energy, which can not only compromise the performance and lifetime of these source electronic components, but also interfere with the function of other nearby components. To efficiently dissipate heat and minimize problems associated with electromagnetic interface (EMI), thermal conducting materials (TCMs) with the combination of high thermal conductivity and excellent EMI shielding performance are urgently needed.

Graphene, the newly discovered two-dimensional (2D) carbon allotrope, possesses both extreme thermal conductivity of ≈5000 W m^{-1} K^{-1} and high electrical conductivity of ≈6000 S cm^{-1}.[1,2] These unique properties make it a new alternative for excellent TCMs and EMI shielding materials. Early studies focused on dispersing graphene into a polymer matrix to enhance the effective thermal and electrical conductivity of the composite.[3–5] However, only modest improvements in thermal performance were achieved due to high thermal interface resistance between graphene and the matrix.[6] Indeed only a low value of ≈2 W m^{-1} K^{-1} was achieved by adding ≈10 wt% of graphene to the polymer matrix. Higher value (~5–10 W m^{-1} K^{-1}) has also been reported by further increasing the graphene loading (>20 wt%),[5,7] however on the cost of the mechanical properties of the composites due to the serious agglomeration. As to EMI shielding, despite ≈5–15 wt% loading of graphene could endow the composites with high EMI shielding effectiveness (SE) of ≈20 dB,[8] the sample thickness of ≈1–3 mm makes them impossible for portable device hardware, such as iPhone and iPad. Therefore, designing new ultrathin graphene-based materials for high-performance TCMs with efficient EMI shielding is becoming an urgent challenge to be addressed.

Graphene oxide (GO), the most accessible precursor of graphene, are of great interest to serve as new building blocks to produce macroscopic materials due to its good dispersion in water and polar organic solvents.[4,9–13] For example, it has been demonstrated that GO sheets could be easily assembled into ultrathin GO films with a layered structure by solution processes.[4,11–14] After being thermal annealed up to high temperatures (≈1000 °C), most oxygen could be removed but structural defects still remained on such thermally reduced graphene film.[15–17] In order to full repair these defects, the post-treatment of reduced graphene film under graphitization condition has been suggested by some recent work, and the as-obained graphitized film possessed continuous oriented graphene layers with very few defects.[18,19] We have reason to believe that such macroscopic graphene film shoud display a remarkable combination of excellent thermal and electrical properties, and could be considered as a promising ultrathin TCMs with efficient EMI shielding.

Since graphene film is obtained by graphitization of GO film under insert gases, the facile and large-scale production of GO film is distinctly a dominant factor in mass-producing graphene film. To date, several methods have been developed for preparation of GO film, including vacuum filtration, spin-coating, centrifugal evaporating, electrophoretic deposition, and interface self-assembly,[4,11–14] while the need of special conditions, such as vacuum, electrodes, or centrifugation, limits the scalability of resulting films. In the case of wet GO film generated, a separation and post-drying process is required, which is

B. Shen, Prof. W. T. Zhai, Prof. W. G. Zheng
Ningbo Key Lab of Polymer Materials
Ningbo Institute of Material Technology and Engineering
Chinese Academy of Sciences
Ningbo, Zhejiang province 315201, China
E-mail: wtzhai@nimte.ac.cn; wgzheng@nimte.ac.cn

DOI: 10.1002/adfm.201400079

inconvenient. Moreover, the above methods have difficulty in producing large-area GO film.

In this work, we first demonstrated a facile and large-scale approach to fabricate large-area GO film by direct evaporation of GO suspension under mild heating. After being treated under graphitization condition, the graphite-like graphene film was obtained and the investigation on the thermal conductivity and EMI shielding performance of the resulting graphene film was futher conducted. The final results revealed that graphene film was indeed a novel promising candidate for excellent TCMs with efficient EMI shielding in today's electronic devices.

2. Results and Discussion

Graphite oxide was synthesized by using a modified Hummers method,[20] and GO suspension was prepared by ultrasonic exfoliation of graphite oxide in water. The thickness of GO sheet we prepared was measured as ≈1.1 nm (Figure S1, Supporting Information), indicating the single-layered attribute of suspended GO sheets in water.[13,21] As shown in **Figure 1**A, GO film was fabricated by pouring GO suspension into Teflon dishes and kept evaporation of water under appropriate heating (50–60 °C) until drying (6–10 h). After that, a free-standing, flexible, dark brown GO film was obtained. The thickness could be well controlled from several to several ten microns by adjusting the volume and concentration of GO suspension. More importantly, it can be easily manufactured in a large-area. For example, a GO film up to ≈400 cm^2 was made with a mold of ≈400 cm^2 dish (Figure 1B) and it can be rolled on a plastic drum due to its flexibility (Figure S2, Supporting Information). Since no special conditions or post-drying process are needed, this approach is convenient and cost-effective. Moreover, particularly worth mentioning is that the low-temperature heating (50–60 °C) could be replaced by solar radiation in summer, since strong solar radiation would greatly accelerate the water evaporation, which make our approach more energy-saving. Furthermore, scanning electron microscopy (SEM) observations showed that the surface of such GO film was smooth with a few thin ripples on it (Figure 1D), and the fracture edge of the film (≈4.3 and ≈11.8 μm in thickness) exhibited layer-by-layer nanostructure through almost the entire cross-section (Figure 1E,F), which was very similar to that of GO film prepared by vacuum filtration.[9,12] The mechanism for the formation of such layered structure might be that, as illustrated in Figure 1A, the evaporation of water rises GO concentration in

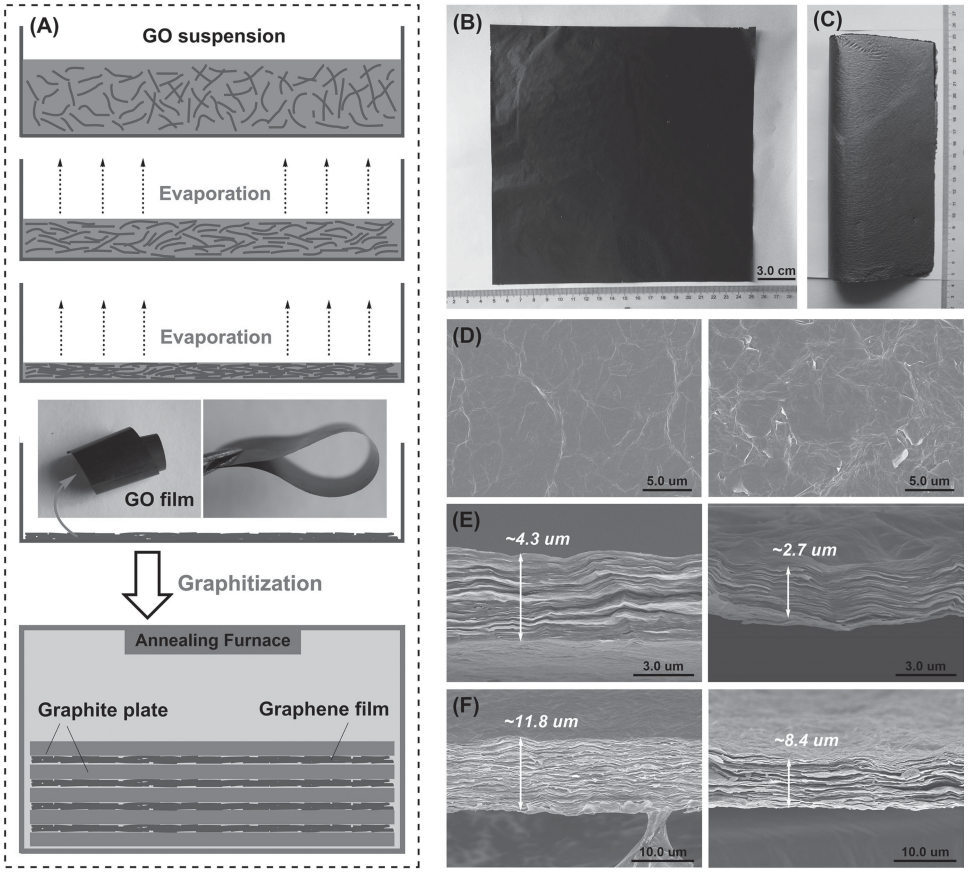

Figure 1. A) Schematic representation of a proposed self-assembly process of GO film by the evaporation of GO suspension, as well as the followed graphitization process. The insert were photographs of a flexible GO film. B) Photograph of a free-standing and dark brown GO film (about 20 cm × 20 cm) flatted on a paper. C) Photograph of a free-standing and shiny metallic GF-2000 (about 20 cm × 20 cm) folded on a paper. D) SEM images showing the surface morphology of GO film (left) and GF-2000 (right). E,F) SEM images showing a layer-by-layer nanostructure in the cross-section of GO film and GF-2000 (with different thickness).

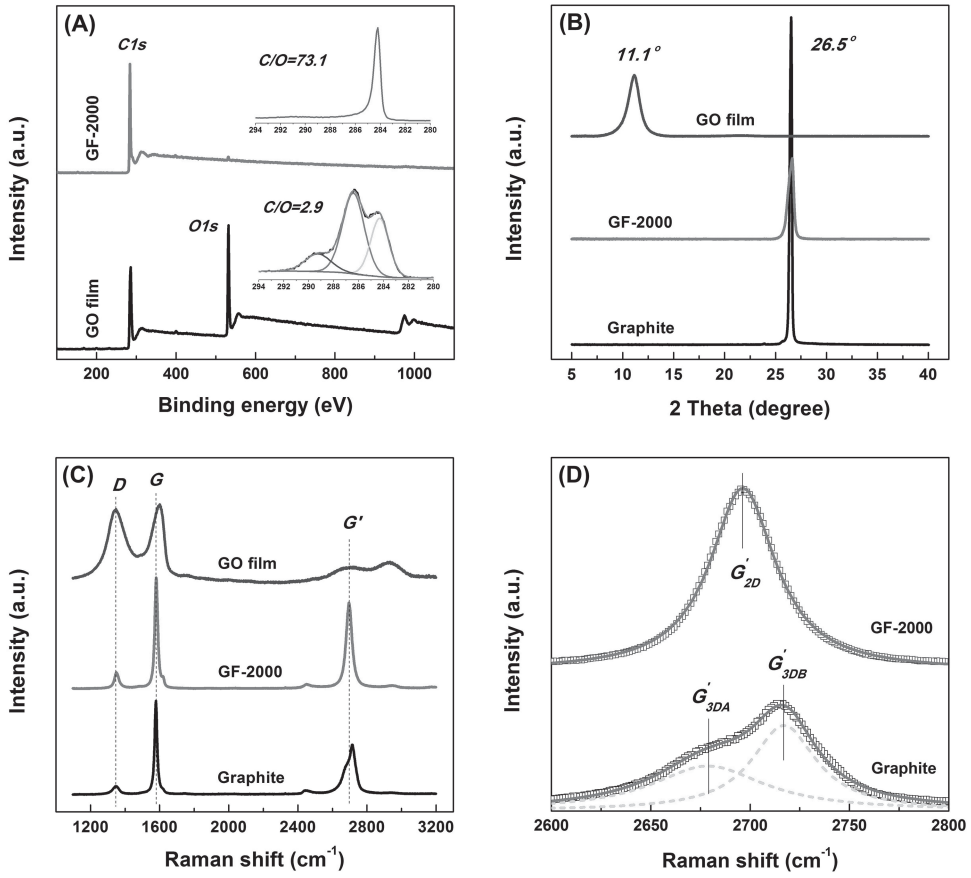

Figure 2. A) High-resolution XPS analysis (C 1s) of GO film and GF-2000 samples. B) XRD patterns of GO film and GF-2000 samples. For comparison, the XRD pattern of pristine graphite is included. All the XRD patterns were recorded at room temperature. C) Raman spectra of GO film and GF-2000 samples with a laser of 532 nm. D) Fitting the measured G′ Raman spectra of GO film and GF-2000 samples. The G'-band goes from one-peak (G'_{2D}) and a two-peak (G'_{3DA} and G'_{3DB}) profile.

the suspension, resulting in a significant increase in the sheet-to-sheet interactions and then making the sheets aligned on top of each other in the ever-growing deposit, thus forming a layer-by-layer nanostructure.

Thermal annealing at 2000 °C was further employed for the reduction and graphitization of GO film, and the as-obtained graphene film was coded as GF-2000. The choosing of graphitization temperature to be 2000 °C was based on previous work which suggested that the crystal defects of GO sheets were substantially repaired at this temperature,[18,19] and higher temperature would only lead to more energy consumption and difficulties in operation. After graphitization, there seemed to be no obvious shrink for GF-2000, while its appearance was changed to black with a shiny metallic luster (Figure 1C), and SEM observation (Figure 1D) also revealed a relative smooth surface with some ripples on it. The cross-sectional SEM views of GF-2000, as shown in Figure 1E,F, exhibited aligned multilayer stacking of graphene layers, with decreased thickness from ≈4.3 to ≈2.7 μm and ≈11.8 to ≈8.4 μm for two samples with different thickness, which should be attributed from the removal of oxygen groups and adsorbed water molecules, resulting in interlaminar consolidation of graphene.[17,19] Such close contact between aligned graphene layers can minimize the barrier for phonon and electron transfer, thereby improving the thermal and electronic properties.

The deoxygenation and interlaminar consolidation was proven by the detailed characterization of X-ray photoelectron spectroscopy (XPS) and X-ray diffraction (XRD) using the thicker film as an example. As shown in the XPS spectra (**Figure 2**A), the C/O atom ratio was remarkably increased from 2.9 of GO film to 73.1 of GF-2000. This value is even higher than that of commercial pristine graphite (28.1; Figure S3, Supporting Information), strongly suggesting a virtually complete elimination of oxygen groups after graphitization. The C1s scan spectra was further fitted into three carbon components with different binding energy: C–C/C=C (≈284.6 eV), C–O–C/C–OH (≈286.5 eV) and carboxyl C=O/O–C=O (≈288.3 eV). It is clear that GO film possessed abundant C–O–C/C–OH (32.5 atom%) and C=O/O–C=O (14.0 atom%) components, however, GF-2000 almost possessed only C–C/C=C component (negligible amounts of oxygen components), verifying the successful removal of epoxyl, carbonyl, and carboxyl functional groups. Because of this, the heat stability of GF-2000 was considerably high, about 400 °C in air as shown in Figure S4, Supporting Information. In the XRD analysis (Figure 2B), the diffraction peak of GF-2000 was shifted from ≈11.1° (GO film) to ≈26.5° (corresponding to the characteristic

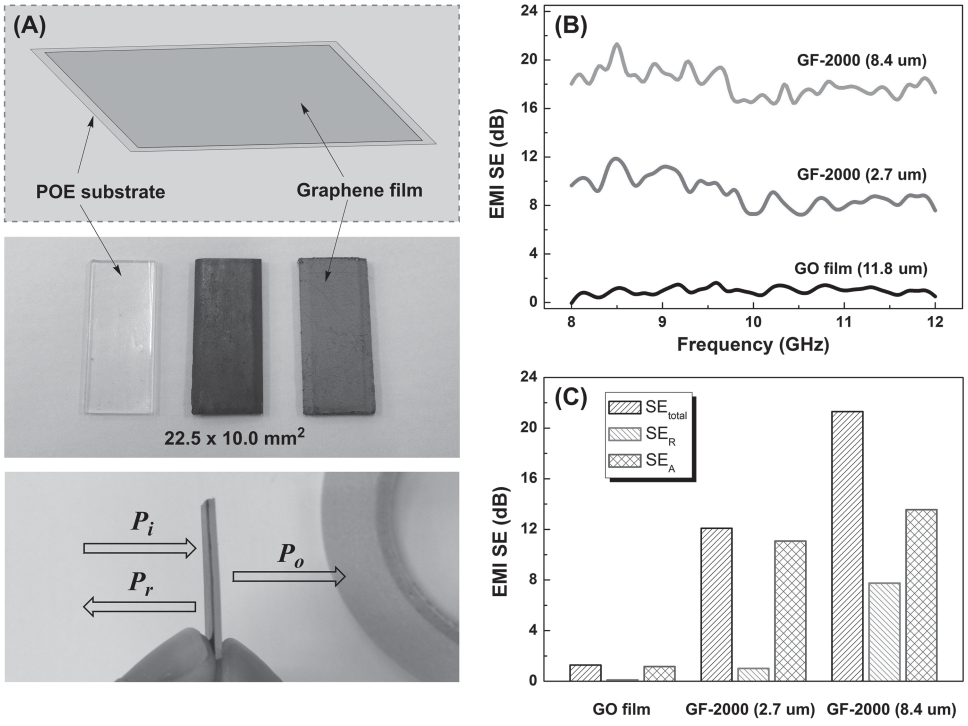

Figure 3. A) Schematic representation of the structure of POE/GF-2000 (or GO film) sample. The EMI SE is defined as the logarithmic ratio of incoming (P_i) to outgoing power (P_o) of radiation. B) the EMI SE as a function of frequency measured in the 8–12 GHz range of GO film and GF-2000. C) SE_{total}, SE_R, and SE_A of GO film and GF-2000 at 8.5 GHz.

peak of pristine graphite), becoming more pronounced and much sharper, which not only exhibited a significant shrinking in interlayer spacing (d_{002}) from 0.80 to 0.33 nm due to the elimination of oxygen groups, but also revealed more regular packing of graphene layers with a longer correlation length due to the coalescence of graphene sheets after graphitization.[18,22]

The effect of graphitization on the structural integrity of graphene sheets was investigated by Raman spectroscopy. As shown in Figure 2C, compared with GO film, the intensity of D-band peak in GF-2000 reduced greatly and the I_D/I_G ratio decreased notably from 0.94 to 0.14, which was quite close to that of pristine graphite, suggesting the extensive repairing of defects created by the attachment of oxygen groups. This was also supported by the significant increased G′-band (≈2700 cm^{-1}) in the second-order Raman spectra. Moreover, the graphitization at 2000 °C would also lead to the coalescence of neighboring graphene sheets into continuous larger sheet, which was confirmed by the experiments carried out by Barreiro et al.[23] Such structural transformation, together with the XPS and XRD results, demonstrated that a graphite-like graphene film has been fabricated from a GO film through the graphitization process. However, unlike pristine graphite with AB Bernal stacking reflected by a highly asymmetric G′-band that can be fitted into two Lorentzian peaks (G'_{3DA} and G'_{3DB}) (Figure 2D), GF-2000 possessed a completely symmetric G′-band that can only be fitted into a single Lorentzian peak (G'_{2D}), revealing the presence of turbostratic stacking between graphene layers due to the random overlaps of GO sheets during the evaporation of GO suspension.[24]

After graphitization, GF-2000 showed excellent electrical conductivity of ≈1000 S cm^{-1}, much higher than that of pristine GO film (≈6.0×10^{-4} S cm^{-1}), because of the structural changes including deoxygenation, better ordered stacking, and defect repairing.[11,18,25] To investigate the EMI shielding performance, the film was attached onto a polyolefin elastomer (POE) substrate using double-sided tape (**Figure 3**A, for the convenience of SE measurement) and the EMI shielding effectiveness (SE) was determined in X-band using the waveguide measurement set up. As shown in Figure 3B, the POE/GO film exhibited hardly any EMI shielding efficiency due to its low conductivity, which also indicated that POE substrate is transparent to electromagnetic waves. In contrast, with the significant increase in conductivity, the EMI SE of the GF-2000 sample (≈2.7 μm) was found to be ≈9.1 dB. Further increase in thickness resulted in higher EMI SE of ≈19.1 dB for the GF-2000 sample (≈8.4 μm). This SE value is close to the target value of EMI SE required for practical application (≈20 dB), indicating GF-2000 (≈8.4 μm) can be used as an effective EMI shielding material. To further clarify the shielding mechanism, the reflection (SE_R) and absorption (SE_A) at 8.5 GHz was calculated from the measured scattering parameters (Figure 3C). It is obvious that both the EM reflection and absorption contributed to the shielding effect but the absorption of EM radiation was the dominant mechanism for EMI shielding of such graphene film.

The superior electrical property implied that GF-2000 would exhibit excellent thermal transport property. Thus, a light flash system (LFA 447 NanoFlash) was employed to determine its in-plane thermal conductivity. As summarized in **Figure 4**,

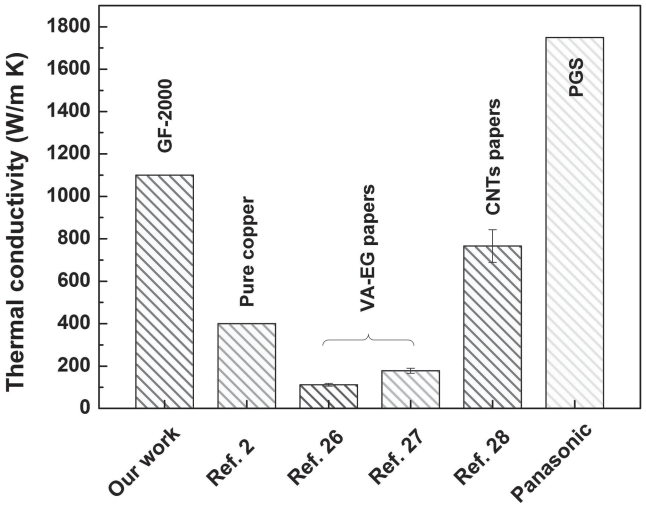

Figure 4. Comparison of the in-plane thermal conductivity of different carbon film (or papers) with the result in this work.

GF-2000 (≈8.4 μm) displayed an outstanding thermal conductivity of ≈1100 W m^{-1} K^{-1} at room temperature, which far exceeds that of pure copper (one of the best metallic heat conductors, ≈400 W m^{-1} K^{-1}),[2] indicating an ideal candidate for excellent TCMs. Moreover, this value was about 6–9 times higher than that of vacuum-assembled exfoliated graphite nanoplatelet (VA-EG) papers (≈112–178 W m^{-1} K^{-1}),[26,27] and also about 30% higher than that of aligned carbon nanotubes (CNTs) papers with high density (≈766 W m^{-1} K^{-1}).[28] We attribute such enhancement to the reduced thermal contact resistance and phonon-boundary scattering resulting from the more compact packing of larger aligned graphene layers with fewer defects in GF-2000 after graphitization.[2,26] Anyway, the thermal conductivity of the film is still much lower than that of individual graphene sheet, possibly due to the inevitable structural defects and interfacial thermal resistance between graphene layers.

Besides the superior electrical and thermal properties, GF-2000 also showed excellent mechanical flexibility and structure integrity during bending. As shown in **Figure 5**A, the film (8.4 μm) was not broken and not cracked even when it was appreciably folded with the tweezers and then pressed with a heavy iron. SEM observation of the crease (Figure 5B) also testified that the graphene layers across this crease were still continuous and free from cracks. As similar to the explanation in foldable CNTs film,[29] we think that the stress during bending is not strong enough to break down the graphene layers, but can make them slip out from the interlamination to accommodate the extension of the outer surface of the film. Here, due to the neighboring coalescence during graphitization, the graphene layers in GF-2000 may become large enough to withstand the slippage to rupture of the film upon bending, or it would crack easily just like some thermal reduced graphene film (≈200–1000 °C) with the characteristic of brittleness.[11,15] To investigate the electrical resistance of GF-2000 under bending, the film was linked with two wires using silver conductive paste and then fixed on two insulating clip (Figure 5C insert). The cycled bending was operated by hand and it was impressive that the resistance did not show an observable increase during 100 times bending (Figure 5C). The good flexibility of GF-2000

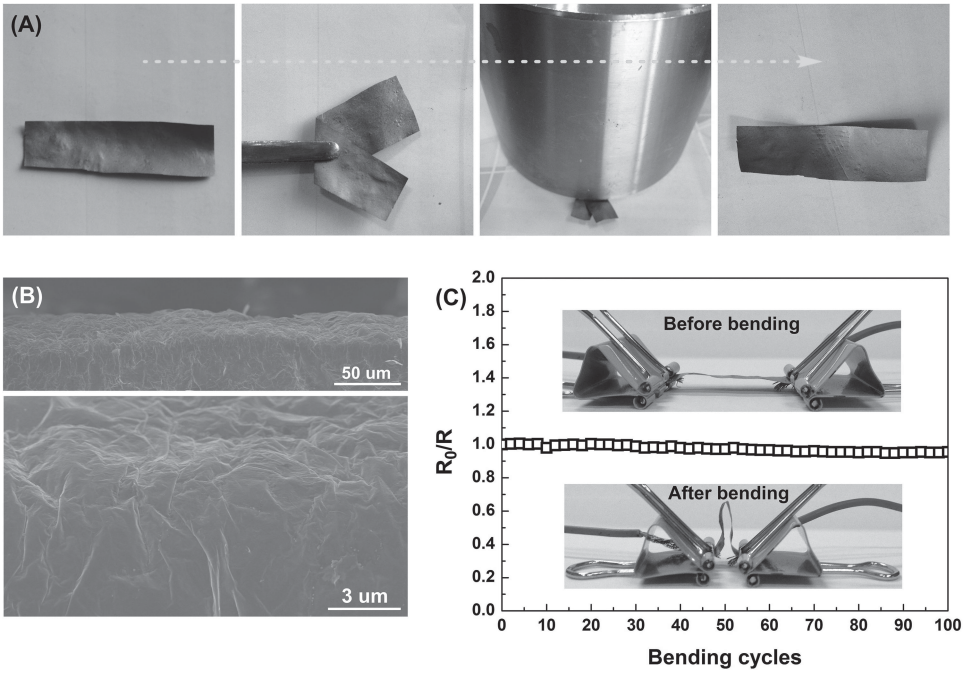

Figure 5. A) Photographs of a folding process of GF-2000 (8.4 μm). It was clear that the film was not broken and not cracked after the folding. B) SEM images of the crease on the outer side of a folded GF-2000 (8.4 μm). C) Resistance change of a GF-2000 (8.4 μm) with bending test. Inset shows the unfolded (above) and folded film (below).

together with the stable resistance suggested that they can be easily adhered to many kinds of surfaces without leading to any damage.

Furthermore, it is noteworthy that there are some commercial flexible graphite films with electrical and thermal conductivity as high as ≈10 000 S cm^{-1} and ≈1750 W m^{-1} K^{-1}, such as PGS from Panasonic. However, they are produced by carbonizing and graphitizing a polymer film such as polyimide,[30] and it has disadvantages that the film is easily broken concomitantly with shrinkage in the carbonization step and the graphitization at a temperature of 2800 °C or more for a long period of time involves huge energy consumption and difficulties in operation. As for our graphite-like graphene film, since graphite oxide has exceptionally low cost and can easily assemble into films by solution processes, the raw material (GO film) are low cost. Moreover, the carbonization step can be omitted and the graphitization temperature can be relatively reduced. The film would also not be broken due to the non-shrinkage during graphitization. Therefore, although the promising results reported here are not as good as the PGS, we still propose that graphitization of GO film could be considered as a new alternative way to produce graphite-like film for excellent TCMs.

3. Conclusions

In summary, we have reported a facile method to fabricate large-area GO film by direct evaporation of GO suspension under mild heating. After graphitization, the resulting graphene film exhibited a graphite-like structure, and possessed excellent EMI SE (around 20 dB) and in-plane thermal conductivity (≈1100 W m^{-1} K^{-1}), indicating that the graphitization of GO film could be considered as a new alternative way to produce excellent TCMs with efficient EMI shielding.

4. Experimental Section

Material Preparation: Graphite oxide was prepared by using a modified Hummers method from natural graphite with a mean size of 35 μm (Qingdao Huatai Lubricant Sealing S&T).[20] The suspension of GO sheets was obtained by ultrasonic exfoliation of the prepared graphite oxide in distilled water, followed by mild centrifugation at 2000 rpm for 10 min to remove non-exfoliated sheets. Then, GO film was fabricated by pouring GO suspension into Teflon dishes and kept evaporation of water under appropriate heating (50–60 °C) for film formation until drying (6–10 h). After peeled from the substrate, a free-standing, flexible, dark brown GO film was obtained. Finally, the GO film was graphitized at high temperature (2000 °C) for 1 hour in a graphite furnace under argon flow. Once the time was over, the sample was cooled down to room temperature while the same argon flow.

Characterization: Scanning electron microscopy (SEM) observation was performed with a Hitachi S-4800 field emission SEM at an accelerating voltage of 4 kV. XPS analysis was carried out a Kratos AXIS ULTRA Multifunctional X-ray Photoelectron Spectroscope using Al (mono) Kα radiation under 1.2×10^{-9} Torr. The diffraction behavior was studied using a Bruker AXS X-ray diffractometer with CuKa radiation at a generator voltage of 40 kV and a generator current of 40 mA. Raman spectra were excited with a laser of 532 nm and record with Labram spectrometer (Super LabRam II system). The electrical conductivity was measured using a standard four-probe method on a Napson Cresbox Measurement System. The EMI SE was measured at room temperature in the frequency range of 8–12 GHz using a WILTRON 54169A scalar measurement system. The samples were cut to rectangle plates with a dimension of 22.5 mm × 10.0 mm to fit the waveguide sample holder. Values of thermal conductivity was caculated from the equation $\lambda = \alpha \times C_p \times \rho$, where λ, α, C_p, and ρ reprensent thermal conductivity, thermal diffusivity, heat capacity, and material density, respectively. The thermal diffusivity and heat capacity of the sample was simultaneously measured by a light flash system (LFA 447 NanoFlash). Density is calculated from sample weight and dimensions.

Supporting Information

Supporting Information is available from the Wiley Online Library or from the author.

Acknowledgements

The authors are grateful to the National Natural Science Foundation of China (Grants 51003115), and Ningbo Key Lab of Polymer Materials (Grant No. 2010A22001) for their financial support of this study.

Received: January 9, 2014
Revised: March 6, 2014
Published online: April 14, 2014

[1] a) A. A. Balandin, S. Ghosh, W. Bao, I. Calizo, D. Teweldebrhan, F. Miao, C. N. Lau, *Nano Lett.* **2008**, *8*, 902; b) X. Du, I. Skachko, A. Barker, E. Y. Andrei, *Nat. Nanotechnol.* **2008**, *3*, 491.
[2] A. A. Balandin, *Nat. Mater.* **2011**, *10*, 569.
[3] a) S. H. Song, K. H. Park, B. H. Kim, Y. W. Choi, G. H. Jun, D. J. Lee, B.-S. Kong, K.-W. Paik, S. Jeon, *Adv. Mater.* **2013**, *25*, 732; b) L. M. Veca, M. J. Meziani, W. Wang, X. Wang, F. Lu, P. Zhang, Y. Lin, R. Fee, J. W. Connell, Y.-P. Sun, *Adv. Mater.* **2009**, *21*, 2088; c) M. A. Raza, A. Westwood, A. Brown, N. Hondow, C. Stirling, *Carbon* **2011**, *49*, 4269; d) X. Tian, M. E. Itkis, E. B. Bekyarova, R. C. Haddon, *Sci. Rep.* **2013**, *3*, 1710.
[4] Y. Xu, H. Bai, G. Lu, C. Li, G. Shi, *J. Am. Chem. Soc.* **2008**, *130*, 5856.
[5] a) K. M. F. Shahil, A. A. Balandin, *Nano Lett.* **2012**, *12*, 861; b) S. Ganguli, A. K. Roy, D. P. Anderson, *Carbon* **2008**, *46*, 806.
[6] a) Q. Li, C. Liu, S. Fan, *Nano Lett.* **2009**, *9*, 3805; b) R. Haggenmueller, C. Guthy, J. R. Lukes, J. E. Fischer, K. I. Winey, *Macromolecules* **2007**, *40*, 2417.
[7] A. Yu, P. Ramesh, M. E. Itkis, E. Bekyarova, R. C. Haddon, *J. Phys. Chem. C* **2007**, *111*, 7565.
[8] a) J. Liang, Y. Wang, Y. Huang, Y. Ma, Z. Liu, J. Cai, C. Zhang, H. Gao, Y. Chen, *Carbon* **2009**, *47*, 922; b) J. Ling, W. Zhai, W. Feng, B. Shen, J. Zhang, W. g. Zheng, *ACS Appl. Mater. Interfaces* **2013**, *5*, 2677; c) H.-B. Zhang, W.-G. Zheng, Q. Yan, Z.-G. Jiang, Z.-Z. Yu, *Carbon* **2012**, *50*, 5117.
[9] X. Lin, X. Shen, Q. Zheng, N. Yousefi, L. Ye, Y.-W. Mai, J.-K. Kim, *ACS Nano* **2012**, *6*, 10708.
[10] a) Z. Xu, C. Gao, *Nat Commun* **2011**, *2*, 571; b) O. C. Compton, S. T. Nguyen, *Small* **2010**, *6*, 711; c) Z. Xu, Z. Liu, H. Sun, C. Gao, *Adv. Mater.* **2013**, *25*, 3249; d) Z. Niu, J. Chen, H. H. Hng, J. Ma, X. Chen, *Adv. Mater.* **2012**, *24*, 4144.
[11] H. Chen, M. B. Müller, K. J. Gilmore, G. G. Wallace, D. Li, *Adv. Mater.* **2008**, *20*, 3557.
[12] D. A. Dikin, S. Stankovich, E. J. Zimney, R. D. Piner, G. H. B. Dommett, G. Evmenenko, S. T. Nguyen, R. S. Ruoff, *Nature* **2007**, *448*, 457.

[13] C. Chen, Q.-H. Yang, Y. Yang, W. Lv, Y. Wen, P.-X. Hou, M. Wang, H.-M. Cheng, *Adv. Mater.* **2009**, *21*, 3007.
[14] a) L. J. Cote, F. Kim, J. Huang, *J. Am. Chem. Soc.* **2008**, *131*, 1043; b) X. Li, G. Zhang, X. Bai, X. Sun, X. Wang, E. Wang, H. Dai, *Nat. Nanotechnol.* **2008**, *3*, 538; c) F. Liu, T. S. Seo, *Adv. Funct. Mater.* **2010**, *20*, 1930; d) W. Huang, X. Ouyang, L. J. Lee, *ACS Nano* **2012**, *6*, 10178.
[15] C.-M. Chen, J.-Q. Huang, Q. Zhang, W.-Z. Gong, Q.-H. Yang, M.-Z. Wang, Y.-G. Yang, *Carbon* **2012**, *50*, 659.
[16] a) O. Akhavan, *Carbon* **2010**, *48*, 509; b) C. Mattevi, G. Eda, S. Agnoli, S. Miller, K. A. Mkhoyan, O. Celik, D. Mastrogiovanni, G. Granozzi, E. Garfunkel, M. Chhowalla, *Adv. Funct. Mater.* **2009**, *19*, 2577.
[17] C. Vallés, J. David Núñez, A. M. Benito, W. K. Maser, *Carbon* **2012**, *50*, 835.
[18] R. Rozada, J. Paredes, S. Villar-Rodil, A. Martínez-Alonso, J. D. Tascón, *Nano Res.* **2013**, *6*, 216.
[19] T. Ghosh, C. Biswas, J. Oh, G. Arabale, T. Hwang, N. D. Luong, M. Jin, Y. H. Lee, J.-D. Nam, *Chem. Mater.* **2011**, *24*, 594.
[20] W. S. Hummers, R. E. Offeman, *J. Am. Chem. Soc.* **1958**, *80*, 1339.
[21] Z. H. Ni, H. M. Wang, J. Kasim, H. M. Fan, T. Yu, Y. H. Wu, Y. P. Feng, Z. X. Shen, *Nano Lett.* **2007**, *7*, 2758.
[22] Z. Xu, Y. Zhang, P. Li, C. Gao, *ACS Nano* **2012**, *6*, 7103.
[23] a) A. Barreiro, F. Börrnert, M. H. Rümmeli, B. Büchner, L. M. K. Vandersypen, *Nano Lett.* **2012**, *12*, 1873; b) A. Barreiro, F. Börrnert, S. M. Avdoshenko, B. Rellinghaus, G. Cuniberti, M. H. Rümmeli, L. M. K. Vandersypen, *Sci. Rep.* **2013**, *3*, 1115.
[24] L. M. Malard, M. A. Pimenta, G. Dresselhaus, M. S. Dresselhaus, *Phys. Rep.* **2009**, *473*, 51.
[25] a) H. A. Becerril, J. Mao, Z. Liu, R. M. Stoltenberg, Z. Bao, Y. Chen, *ACS Nano* **2008**, *2*, 463; b) G. Eda, G. Fanchini, M. Chhowalla, *Nat. Nanotechnol.* **2008**, *3*, 270.
[26] J. Xiang, L. T. Drzal, *Carbon* **2011**, *49*, 773.
[27] Q. Liang, X. Yao, W. Wang, Y. Liu, C. P. Wong, *ACS Nano* **2011**, *5*, 2392.
[28] L. Zhang, G. Zhang, C. Liu, S. Fan, *Nano Lett.* **2012**, *12*, 4848.
[29] J. Di, D. Hu, H. Chen, Z. Yong, M. Chen, Z. Feng, Y. Zhu, Q. Li, *ACS Nano* **2012**, *6*, 5457.
[30] M. Murakami, N. Nishiki, K. Nakamura, J. Ehara, H. Okada, T. Kouzaki, K. Watanabe, T. Hoshi, S. Yoshimura, *Carbon* **1992**, *30*, 255.